Backside Localization of Open and Shorted IC Interconnections

Edward I. Cole Jr., Paiboon Tangyunyong, and Daniel L. Barton

Sandia National Laboratories
Electronics Quality/Reliability Center
MS 1081, Albuquerque, NM 87185-1081
Tel. 505-844-1421 e-mail: coleei@sandia.gov
FAX 505-844-2991

ABSTRACT

A new failure analysis technique has been developed for backside and frontside localization of open and shorted interconnections on ICs. This scanning optical microscopy technique takes advantage of the interactions between IC defects and localized heating using a focused infrared laser (λ = 1340 nm). Images are produced by monitoring the voltage changes across a constant current supply used to power the IC as the laser beam is scanned across the sample. The method utilizes the Seebeck Effect to localize open interconnections and Thermally-Induced Voltage Alteration (TIVA) to detects shorts. The interaction physics describing the signal generation process and several examples demonstrating the localization of opens and shorts are described. Operational guidelines and limitations are also discussed.

INTRODUCTION

Open and short circuited interconnections are major IC yield and reliability problems and will increase in importance as the number of interconnection levels and length of interconnections continue to increase. The ability to localize the defects responsible for various failure modes is critical in diagnosing IC failures and implementing corrective action. Today's ICs employ multiple levels of metal that obscure lower conductor levels and flip-chip packaging that make IC frontside examination techniques either difficult or impossible to apply. These problems have driven the development and use of backside IC analysis techniques. Unfortunately, the present suite of backside methods is not totally effective in localizing open and shorted conductors. Existing methods can be time consuming, yield a great deal of superfluous information, and provide only indirect evidence of open and short circuit defects.

One common aspect of many backside IC analysis techniques is the use of infrared light because of Si's relative transparency at infrared wavelengths. Backside optical microscopy, photon emission microscopy [1], and transistor logic state mapping [2] use infrared light to either stimulate the IC or monitor reflected/transmitted signals. Backside Optical Beam Induced Resistance Change (OBIRCH) [3] has been shown recently to localize shorted conductors, but the detection sensitivity is limited.

To overcome the limitations of existing techniques, we have developed a new scanning optical microscopy (SOM) imaging method which directly localizes both open and shorted interconnections of ICs from the front and backside of the Si substrate. The method uses a scanned infrared laser source to produce localized thermal gradients in the IC interconnections. The effects of the thermal gradients on IC power consumption are detected by monitoring the voltage fluctuations of the IC power supply voltage (V_{DD}) with the IC biased using a constant current power supply. Open conductors are detected using the Seebeck Effect to change the power demands of the IC. Conductor short sites are localized using the resistance change described by OBIRCH and the enhanced detection sensitivity provided by constant current biasing. The Thermally-Induced Voltage Alteration (TIVA) images can localize short sites in a single, entire die field of view image.

The laser beam and defect interaction physics used to generate Seebeck Effect Imaging (SEI) and TIVA images are described. The data acquisition system, protocols for image collection, and areas for system improvement are also discussed. Several examples demonstrating the utility of thermal gradient effects for localizing open and shorted interconnections from the frontside and backside of ICs are presented.

IMAGING SYSTEM

A block diagram of the SOM system used for SEI and TIVA imaging is shown in Fig. 1. The SOM is a Zeiss Laser Scan Microscope. A 1340 nm, Nd:YVO_4 laser illumination source and a Ge diode photo-detector produce reflected light images. A Keithley 238 source measurement unit provides electrical stimulus to the IC and an Ithaco 1201B voltage amplifier detects voltage variations in V_{DD}. The amplifier is operated in the ac-coupled mode so that only the variations in V_{DD} are used to make the images.

The SOM and system components are similar to those described for backside LIVA imaging [2], with the important change in laser wavelength to 1340 nm. The photocurrent effects from electron-hole pair generation by the 1064 nm laser used in LIVA produce signals 1 to 2 orders of magnitude larger than the SEI and TIVA signals and must be avoided. The 1340 nm wavelength illumination source eliminates the LIVA signal because the energy of the photons is below that of the Si indirect band-gap. In practice, when using amplification gains of 5000 or more on the Ithaco we observed some LIVA signals. The specifications for our laser indicate that < 1% of the laser power may be at a 1047 nm wavelength. To eliminate the unwanted LIVA signals, a 4th order, long wavelength pass filter was placed in the beam path as shown.

Typical image scan times of 4 to 8 seconds per frame were used. The relatively long scan times were required to compensate for the loss in amplifier bandwidth at high gains. Line averaging of 8 to 16 lines was also used to improve the image signal to noise ratio. For particularly weak signals, image averaging of 4 to 16 frames was also performed as indicated in the text. System improvements

DISCLAIMER

DISCLAIMER

Portions of this document may be illegible electronic image products. Images are produced from the best available original document.

that would increase SEI and TIVA signal strength are described in the Future Research section.

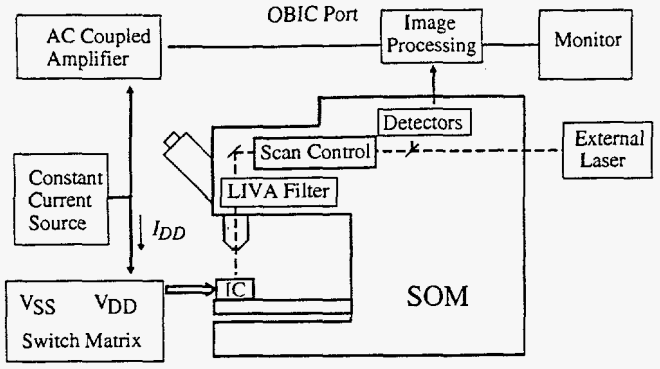

Fig. 1. SOM system used for SEI and TIVA.

SEEBECK EFFECT IMAGING

Thermal gradients in conductors generate electrical potential gradients with typical values on the order of μV/K [4]. This is known as thermoelectric power or the Seebeck Effect and refers to the work of Thomas Johann Seebeck (1770-1831)[5]. The most common application of thermoelectric power is the thermocouple, which uses the difference in thermoelectric voltages of two different metals to measure temperature (Fig. 2.) For IC analysis, the effect has been demonstrated as a means to localize voiding in metal test patterns [6]. If an IC conductor is electrically intact and has no shorts, the potential gradient produced by localized heating is readily compensated for by the transistor or power bus electrically driving the conductor and essentially no signal is produced. However, if the conductor is electrically isolated from a driving transistor or power bus, the Seebeck Effect will change the potential of the conductor. This change in conductor potential will change the bias condition of transistors whose gates are connected to the electrically open conductor, changing the transistors' saturation condition and power dissipation. An image of the changing IC power demands displays the location of electrically floating conductors.

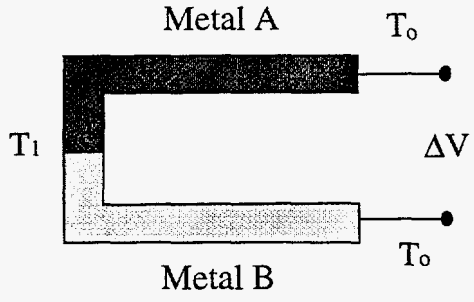

Fig. 2. Elementary thermocouple.

The results of thermal modeling at Sandia showed that a focused 1340 nm laser will produce about a 1 °C/mW temperature change in a Si substrate. At present a 120 mW, single mode, polarized laser is used for thermal stimulus. The transmission efficiency of our SOM (about 3% to 25% depending upon the objective lens) indicates that thermal gradients on the order of 4 °C to 30 °C can be produced, creating potential variations in the 1's to 10's of μV. Essential to SEI localization of open interconnections is detection of the small changes in transistor gate voltages with thermal gradients. Detection of the small variation in transistor bias condition is accomplished by using constant current biasing of the IC. The Light- and Charge-Induced Voltage Alteration (LIVA and CIVA) imaging techniques [2, 7, 8] and transient voltage (v_{DDT}) test method [9] have shown that monitoring the supply voltage to the IC with constant current biasing conditions provides an extremely sensitive method for detection of subtle changes in the IC power demand. Fig. 3 displays a comparison of IC current increase using constant voltage biasing to IC voltage decrease using constant current biasing for a CMOS ACIC. For example, a power demand change that would produce a 15 nA change in I_{DDQ} at a constant voltage will produce a 300 mV change in V_{DDQ} at constant current. For very low power CMOS devices, IC power changes corresponding to a supply current increase of 100 pA for a constant supply voltage have been shown to produce a 2 V supply voltage decrease for constant supply current biasing. This sensitivity is critical in detecting the potential gradients produced by the Seebeck effect. Typical amplifier gains used for SEI in this work range from 5000 to 10,000. For our system this indicates V_{DD} changes on the order of 0.1 mV. The current changes with constant voltage biasing were too small to be detected with our present system. The 1340 nm wavelength is suitable for effective Si transmission and conductor heating, will not produce electron-hole pairs (avoids photocurrent effects), and yields reasonable spatial resolution in a reflected light image. Note that changing the voltage of open conductors that do not drive transistor gates (for example an open power bus) may not change the power demand of the IC and will therefore not be detected using SEI.

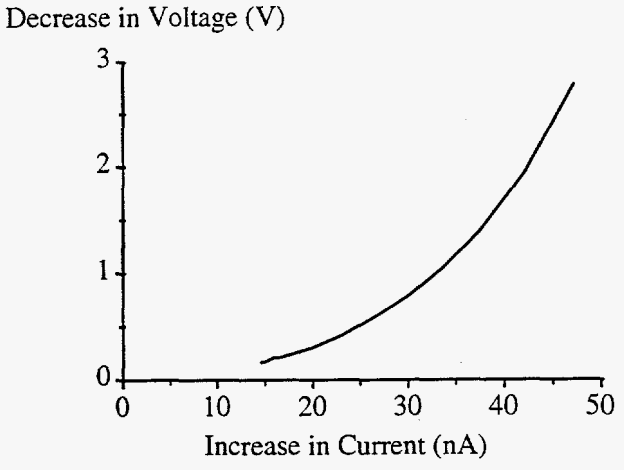

Fig. 3. Sensitivity comparison of constant voltage and constant current biasing under the same stimulus.

The SEI signal is produced by heating the open conductor which occurs even if the scanned thermal probe is larger than the conductor. The spatial resolution of SEI will be limited by the 1340 nm wavelength, however the detection sensitivity of SEI image contrast depends on the conductor being examined and not on the probe size. Therefore, the image of the open interconnection may appear larger than the actual conductor, but will effectively localize the open signal path.

TIVA IMAGING

Localized thermal gradients can also detect shorted IC conductors. Shorted conductors cause increased IC power consumption when the shorted conductors are at different electrical potentials, i.e. a short between V_{DD} and V_{SS}. The power consumption will depend upon the resistance of the short site and its location in the circuit. A low resistance V_{DD} to V_{SS} power bus short may dissipate more power than two shorted signal lines. As a laser is scanned over an IC with a short circuit, laser heating changes the resistance of the short when it is illuminated, changing the IC power demand. The resistance change can be expressed as [10]:

$$\rho = \rho_o (1 + \alpha(T-T_o))$$

where ρ is the resistivity, ρ_o is the resistivity at T_o, α is the temperature coefficient of resistivity, T is the temperature and T_o is the reference temperature.

It has been found that thermally-induced power changes are usually greater for shorted signal lines than power busses. This results from signal line voltage fluctuations altering transistor gate voltages, producing the same amplification effect observed in CIVA and SEI. This resistance change with localized heating is the basis for the OBIRCH technique [3]. For OBIRCH, the change in IC power consumption is detected by an IC current change with constant voltage bias, yielding limited detection sensitivity [3]. The constant supply current biasing approach achieves greater sensitivity and a TIVA image is produced localizing the short.

Therefore, using the same IC biasing and laser stimulus, both open and shorted conductors can be localized from the front and backside of an IC.

IMAGING EXAMPLES

Seebeck Effect Imaging

Fig. 4(a) is an SEI image from the frontside of an IC. The IC is a radiation-hardened, 4 μm metal, 3 μm polysilicon, CMOS version of an Intel 8085 microcontroller manufactured at Sandia using a single level metal process. The open site was produced by laser ablation. Fig. 4(b) is a reflected light image of the same field of view for registration. Note that the entire die is examined in a single image. The floating conductor path and the transistors controlled by the conductor are visible in Fig. 4(a). The transistor diffusions appear bright compared to the open conductor contrast. We believe the bright signals result from the diffusion to well thermopower difference, changing the voltage of gates downstream of the floating gate transistors when heated. In effect, the junction region is acting like a small thermocouple.

Fig. 5(a) shows the same device in Fig. 4 at higher magnification. The laser ablation site is indicated by an arrow. The SEI images are reminiscent of CIVA images showing open conductors but with reduced signal strength.

An SEI section of the floating conductor in Fig. 4 is displayed at higher magnification in Fig. 6(a). Contrast enhancement and superposition with the reflected light image localize the open conductor.

Somewhat surprising is the fact that we do not see a contrast change in metal-polysilicon interconnections on this older Sandia technology. (In later examples we do observe contrast in the electrically floating metal-polysilicon interconnections.) The metal conductors in this older technology were processed without Cu doping of the Al. The difference in processing appears to have resulted in a much smaller thermopower difference than seen in other interconnections below.

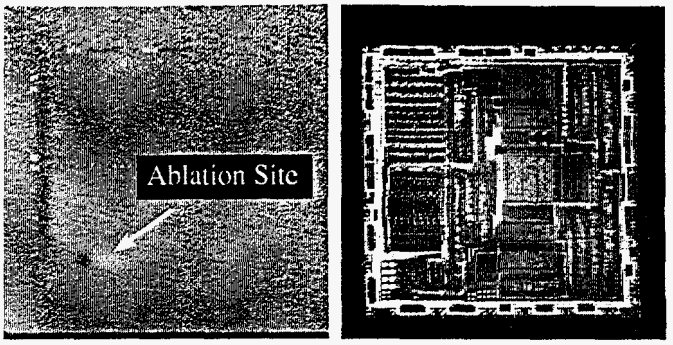

(a) (b)

Fig 4. (a) Frontside SEI image of a floating conductor. (b) Reflected light image with the same field of view for reference.

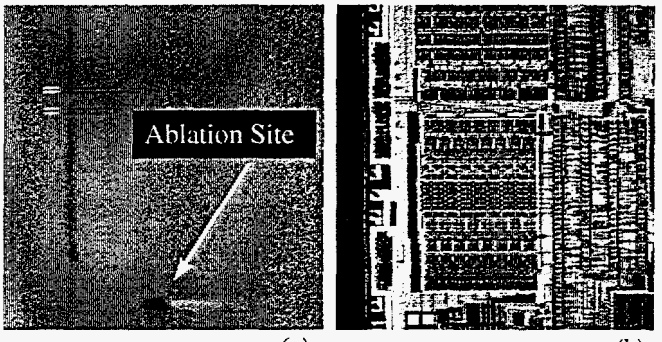

(a) (b)

Fig 5. (a) Higher magnification frontside SEI image of the floating conductor in Fig. 4. (b) Reflected light image of the same field of view for reference.

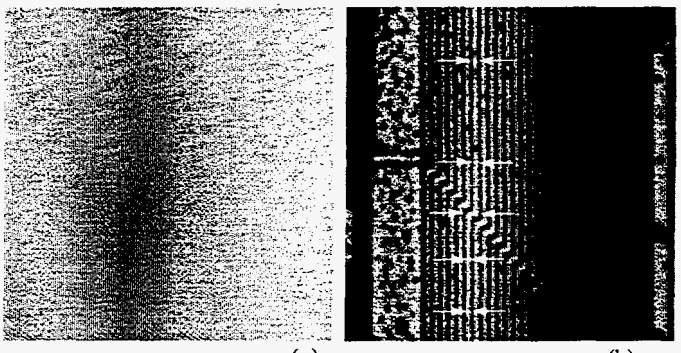

(a) (b)

Fig. 6. (a) Frontside SEI image section of a floating conductor. (b) Superposition of the image in Fig. 6(a) and a reflected light image of the same field of view.

Fig. 7 is another frontside SEI example of a open conductor on a radiation-hardened CMOS version of an Intel 80C51 microcontroller manufactured at Sandia using a two-level metal, 1.25 μm process. The open was created with a focused ion beam (FIB). Fig. 7(a) shows the open site with the long wavelength pass filter in place. Fig. 8(a) displays the same open site with the filter removed. The blurred contrast visible in Fig. 8(a) is a LIVA signal produced from the 1047 nm component of the laser. The signal appears blurred

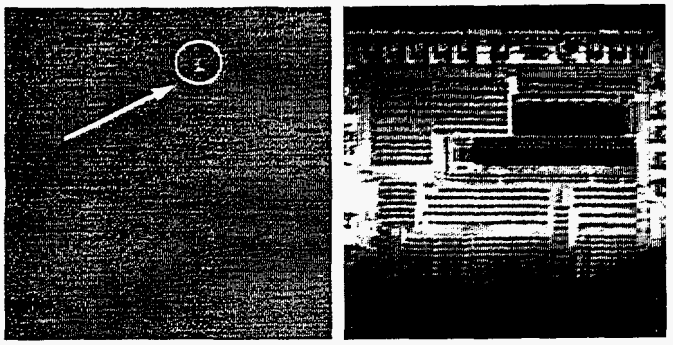

(a) (b)

Fig. 7. (a) Frontside SEI image and (b) reflected light image of an open conductor on a microcontroller.

because the focus is optimized for the 1340 nm wavelength. The filter was left in place for subsequent images to eliminate the LIVA signals.

A higher magnification view of the open conductor shown in Figs. 7 and 8 is shown in Fig. 9(a). The arrow indicates the FIB open site. Note that not only is the open conductor visible, but a weaker and somewhat diffuse signal can also be seen from the conductor and gates **beneath** the upper metal-2 power bus. The contrast from the lower structures indicates that the thermal gradient on the surface of the metal-2 has propagated through the metal and interlevel dielectric to the metal-1 and polysilicon conductors underneath. This thermal conduction is consistent with the modeling work shown recently by Ferrier [11] for subsurface, heat producing defects.

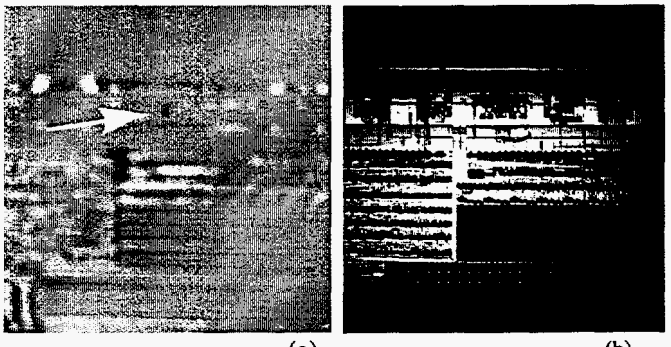

(a) (b)

Fig. 8. (a) SEI and (b) reflected light image pair similar to Fig 7 with the long wavelength pass filter removed. The blurred contrasts in Fig. 8(a) are from LIVA signals. The SEI signal is indicated by the arrow.

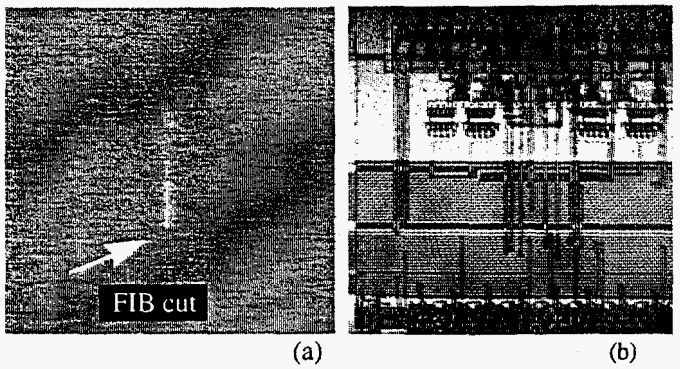

(a) (b)

Fig. 9. Higher magnification (a) SEI and (b) reflected light views of the open conductor in Fig. 7.

The microcontroller in Fig. 9 could be clocked to a different state where a much stronger contrast was observed. This contrast (Fig. 10) appears to be originating from under the power bus but could not be localized further from the frontside of the IC.

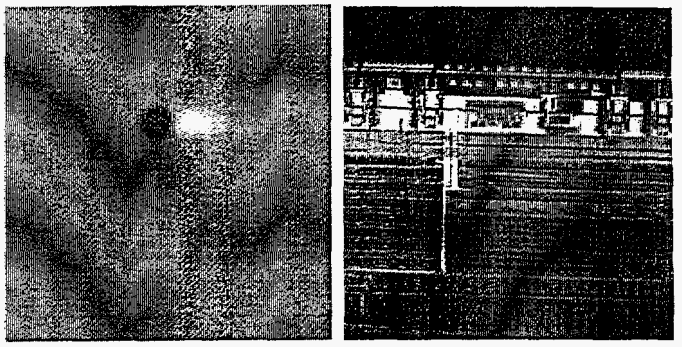

(a) (b)

Fig. 10. (a) Strong SEI contrast signal produced by clocking the microcontroller and (b) reflected light image.

Backside SEI was performed using the same 1340 nm wavelength laser for stimulus. The signal strength is reduced for backside examination because of absorption by doped Si. Fig. 11 shows the percent transmission as a function of wavelength and *p*-doping concentration for 625 μm of Si [12]. Heavier doping will increase the absorption. Thinning of the sample improves signal strength. The percent transmission of infrared wavelengths is expressed by [12]:

$$\%T = \frac{(1-r)^2 e^{-\alpha d}}{1-r^2 e^{-2\alpha d}} \times 100\%$$

where %T is the percent transmission, r is the reflection coefficient, α is the absorption coefficient, and d is the Si thickness. Decreasing the thickness can dramatically increase the %T and therefore the SEI signal. No thinning, beyond backside exposure, was performed on the samples used in this work.

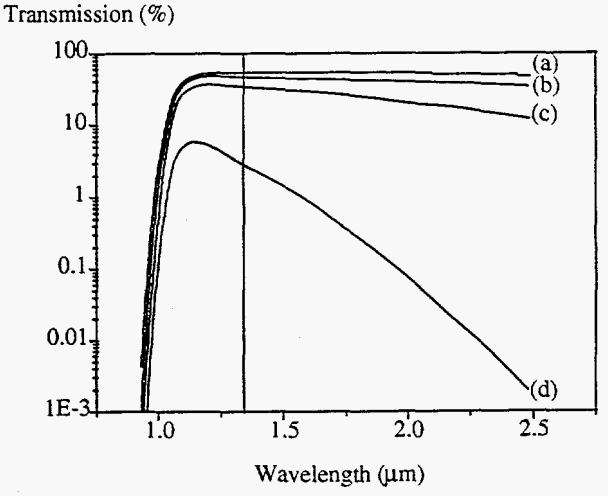

Fig. 11. Percent transmission of light through 625 μm of *p*-doped Si having doping concentrations of (a) 1.5×10^{16}, (b) 3.3×10^{17}, (c) 1.2×10^{18}, and (d) 7.3×10^{18} cm^{-3}. The 1340 nm wavelength is marked by a vertical line.

Fig 12 is a backside SEI imaging example of a floating conductor. The floating conductor was produced by laser ablation. The IC is a low power CMOS ASIC manufactured at Sandia in a 4 μm metal, 3 μm polysilicon process. The sample was potted in epoxy and planar lapped to expose the back of the die. The arrow indicates the laser ablation site. The floating conductor path from the open site to the driven transistor gate can be seen. Note that the CMOS logic gates can be seen as a weak background signal (Fig. 12(a)). These are not produced by a LIVA effect, but are probably produced by directly heating the diffusions using the 1340 nm laser. This imaging of the logic states was observed only on this low power ASIC. We believe that the signal originates from the thermocouple effect seen earlier and exists on all samples examined, but is too weak to be seen on any of the other devices examined other than this low power IC.

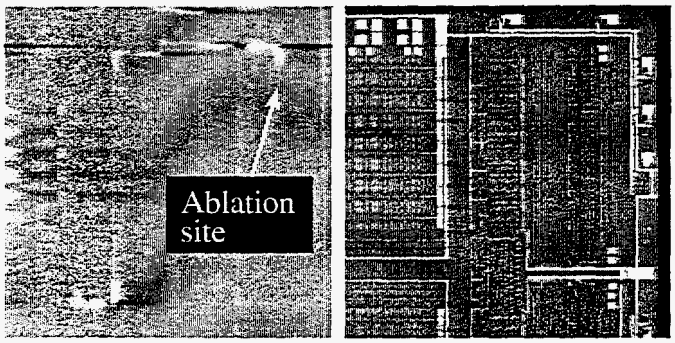

Fig. 12. (a) Backside SEI imaging example of a floating conductor. (b) Reflected light micrograph of the same field of view.

A higher magnification backside view of the laser ablation site is shown in Fig. 13. Fig. 13(a) is an average of 4, 8 second per frame scans, each scan having 16 line averaging. The open site is indicated by the arrow. In addition to the floating conductor, there are two features of note in Fig. 13(a). First, a "halo" of image contrast is present about the laser ablation site. In the reflected light image (Fig. 13(b)) we see that this area is unpopulated Si. The lateral, thermal conduction efficiency of Si is relatively high. As areas of the Si surface are heated by the focused laser beam with no intervening structures to absorb the heat, the floating conductor is heated and the Seebeck Effect occurs. The resulting effect is a less localized SEI image due to thermal spreading in the Si. A second feature of Fig. 13(a) is the strong contrast in the region where the conductor goes over the field oxide and *p*-well of logic gates. We believe that the these features reduce thermal loss through the Si and increase the thermal gradient along the conductor. Contrast changes at the polysilicon-metal interconnections are not visible in Fig. 13(a). The IC was produced in the process described earlier that does not use Cu doping of the Al.

Fig. 14(a) is a backside SEI example of the open conductor shown in Figs. 7 and 9. Note that even with a relatively poor polish (Fig 14(b)) the open site can be identified. At higher magnification the open FIB site and floating conductor can be seen (Fig. 15(a)). Fig. 15(a) is an average of 16, 8 second per frame scans, each scan having 16 line averaging. Relatively strong contrasts were produced by the metal-1 (Cu doped) to polysilicon interconnections. Observe that the contrast changes from dark, to bright, to dark at metal-poly, poly-metal. and metal-poly interconnections respectively. We believe this is due to a thermocouple effect between the polysilicon and metal conductors.

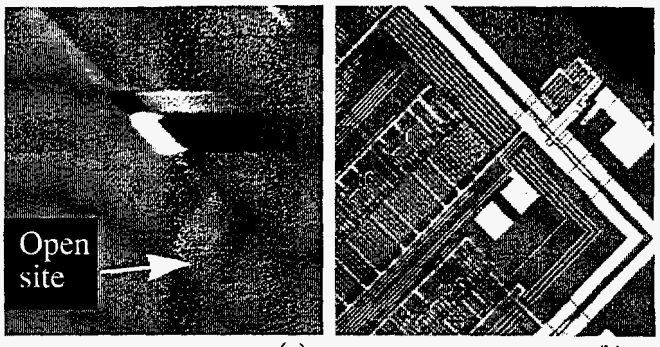

Fig 13. (a) Higher magnification backside SEI and (b) reflected light image pair of the defect shown in Fig. 12.

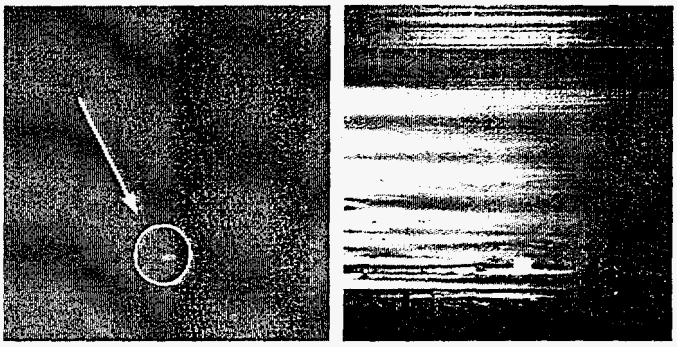

Fig. 14. (a) Backside SEI and (b) reflected light images of the open conductor show in Figs. 7 and 9.

The microcontroller could be clocked to the state similar to that shown in Fig. 10 and imaged from the backside. Fig. 16 is a backside SEI image of this logic state. The signal strength of the contrast site was approximately 2 orders of magnitude greater that the signals in Figs. 14 and 15. The *p*-channel transistor generating the contrast can be identified. The signal is produced as the downstream gates driven by the floating transistor have their voltage changed. We believe that the signal is stronger because of a thermocouple effect between the *p*-diffusion and *n*-well of the floating gate transistor.

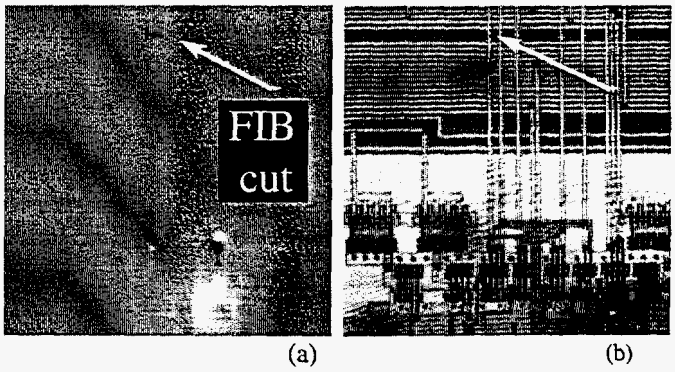

Fig. 15. (a) Higher magnification backside SEI and (b) reflected light images of the open conductor shown in Fig. 14.

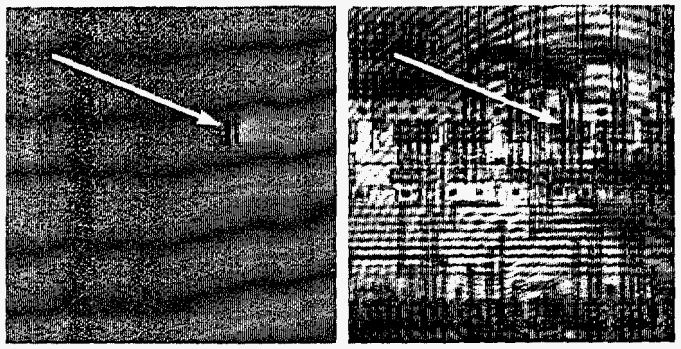

(a) (b)

Fig. 16. (a) Strong backside SEI image contrast from the microcontroller of Fig. 14 clocked to a different logic state. (b) Reflected light image of the same field of view.

TIVA Imaging

Fig. 17 displays a frontside TIVA image example of a FIB produced short on a 3-level metal, 0.5 micron, 256K SRAM. Fig. 18 is a higher magnification view of the memory. The FIB short is the dark, rectangular contrast seen in Fig 18(b). Fluorescent Microthermal Imaging (FMI) [13] identified the bright contrast indicated by the arrow as a heat producing source, but not the additional contrast sites seen in the TIVA image. Subsequent LIVA analysis of the IC with a visible, 5 mW, 543 nm wavelength laser identified the additional contrast sites seen in the TIVA image but not the short site found in the TIVA and FMI images. The spurious TIVA and LIVA contrast sites are transistor diffusions connected to the shorted conductor and are therefore not connected directly to V_{DD} or V_{SS}. We believe that the thermocouple effect seen before changes the voltage of these diffusions and the transistor gates they drive. Similarly, the photocurrents induced by LIVA will have the same effect and produce the similar LIVA contrast sites observed. The heating effects of the 5 mW, 543 nm laser are not significant compared to its electron-hole pair generation.

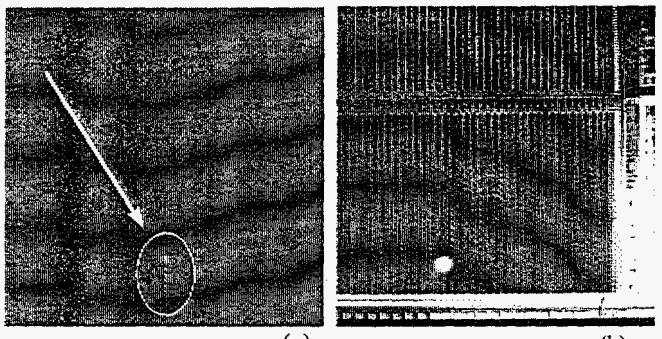

(a) (b)

Fig. 17. (a) Frontside TIVA image of a FIB short on a 256K SRAM. (b) Reflected light image of the same field of view. The bright spot in the bottom of (b) is caused by internal reflection in the SOM.

A frontside TIVA image of an entire, 3-level metal, 0.5 μm, 1 Mb SRAM is shown in Fig. 19. The TIVA short site was identified as a stainless steel particle shorting two signal lines. Fig 20 is a higher magnification view of the short site. The particle causing the short and a small section of the shorted conductors can been seen in Fig 20(a). The particle is visible in Fig 20(b).

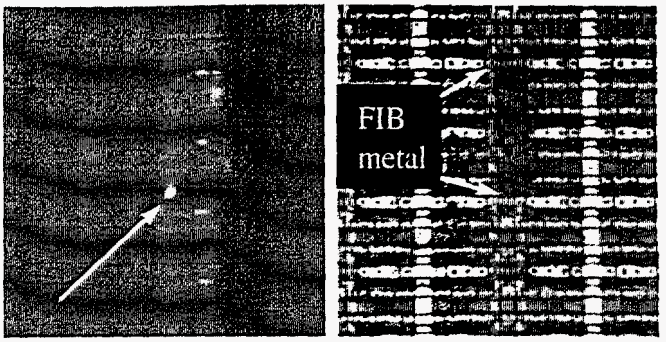

(a) (b)

Fig. 18. Higher magnification frontside TIVA and reflected light images of the FIB short site in Fig. 17. The arrow indicates the hot spot found using FMI. The rectangular FIB deposited metal can be seen in Fig 18(b).

Fig. 21 is a frontside TIVA image of a stainless steel particle short between two signal lines on another 1Mb SRAM. The particle is clearly seen in Fig 21(b), but the spatial resolution is not sufficient to see the individual conductors. The surface of this memory was sealed with epoxy and polished for backside TIVA analysis.

The backside TIVA image acquired is shown in Fig. 22. The arrow highlights a very small TIVA contrast site. Fig. 22a was contrast enhanced to make the small contrast site visible. The SRAM was biased with 4 mA and reached a voltage of 4.6 V. The voltage changes from the TIVA contrast site were about 0.3 mV. No supply current changes were observed using a 5 V constant voltage bias arrangement. Fig. 23 is a higher magnification backside TIVA image of the short site. Note that while the short site is clearly visible in the TIVA image, the particle, now under the metal conductors, cannot be seen in the reflected light micrograph (Fig. 23(b)).

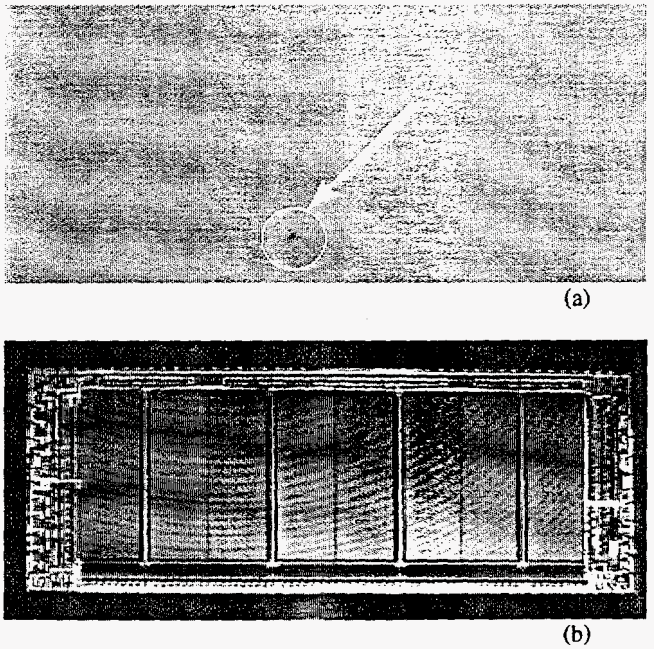

(a)

(b)

Fig. 19. (a) Frontside TIVA image of a 1 Mb SRAM. The arrow indicates the short site. (b) Reflected light image for registration.

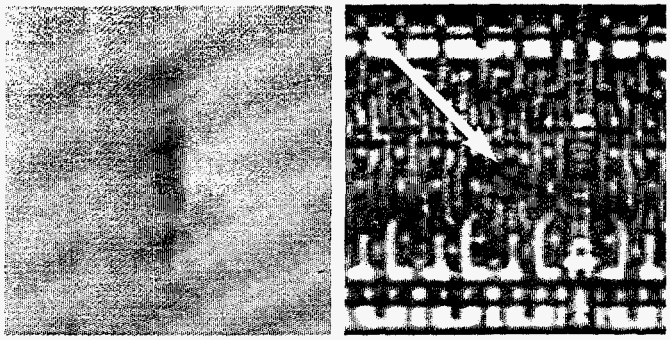

(a) (b)

Fig. 20. Higher magnification frontside TIVA and reflected light image pair of the short site in Fig. 19. The shorting particle can be seen in Fig. 20(b). The blurred appearance of Fig. 20 (b) demonstrates the spatial resolution limitations of imaging with the 1340 nm wavelength laser.

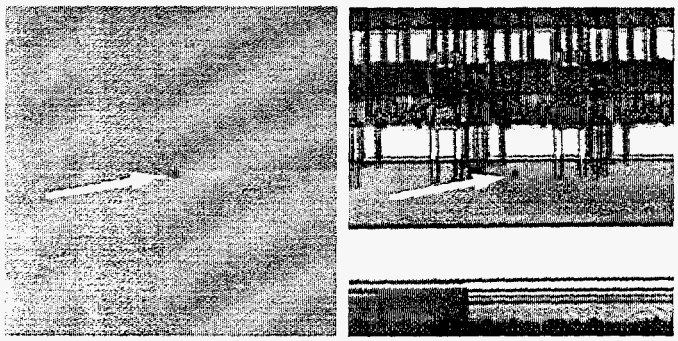

(a) (b)

Fig. 21. Frontside TIVA and reflected light image pair showing a particle short on the 1 MB SRAM.

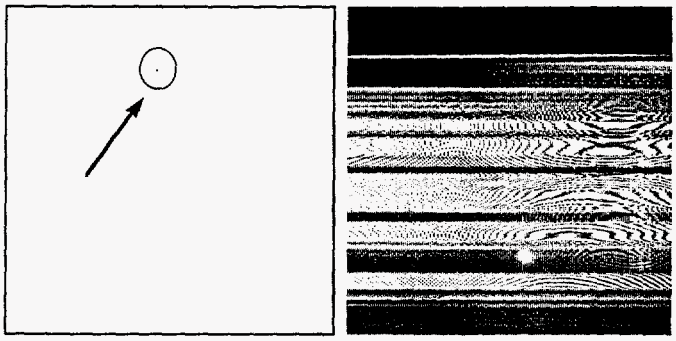

(a) (b)

Fig. 22. (a) Backside TIVA image locating the short on the SRAM from Fig 21. (b) Reflected light image for registration.

FUTURE RESEARCH

A recurring problem in developing the thermal gradient imaging technique to localize open and shorted conductors (particularly with SEI) was the desire for increased signal strength. While averaging somewhat compensates for the weaker signals, further improvements are required to examine higher power ICs and to compensate for substrates with higher infrared absorption.

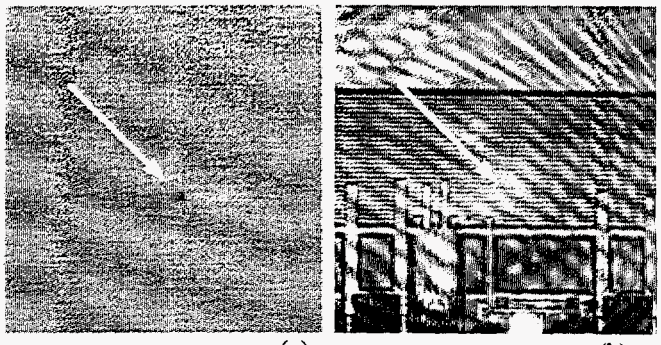

(a) (b)

Fig 23. Higher magnification backside TIVA and reflected light image pair of the short site from Fig 22. Note that the particle cannot be seen from the backside in Fig. 23(b).

We are implementing two improvements to our data acquisition system. First, we are acquiring a higher power (350 mW) laser to replace the 120 mW laser. This alone should increase our signal strength by about 3X. Higher power lasers are available but they are relatively expensive (> $40K) and there are limits to the power that can be transmitted through the SOM optics without damaging the surface coatings.

A second improvement will use a pulsed laser and lock-in amplification of the SEI and TIVA signals. Although Si has a high thermal conductivity, there are limits to how fast a laser pulse can be and still produce a useful change in temperature between pulses. Modeling at Sandia indicates that the time constant for Si surface heating by a focused laser is in the range of 100 to 200 ns. The thermal response of the surface to a 1 MHz modulated laser should produce changes in temperature within 90% of the steady state heating conditions. To pursue the lock-in approach, a 1 MHz optical shutter will be used to convert the 350 mW CW laser to pulse mode. The 1 MHz pulse rate will allow multiple signal samples for each image pixel. (An 8 second per frame scan rate yields a 30 μsec dwell time per pixel for a 512 x 512 pixel image.)

These system improvements should yield greater signal sensitivity and extend the application of the SEI and TIVA techniques.

CONCLUSIONS

The SEI/TIVA technique has been developed as a new, nondestructive analytical method for backside failure analysis. Through backside localization of open interconnections, SEI provides what has been a critical "missing link" in IC analysis capability. The high sensitivity of TIVA yields a practical tool for short localization from both the front and backside of the IC. SEI/TIVA is a powerful new addition to the set of failure analysis tools.

ACKNOWLEDGMENTS

The authors thank Steve Kirch of Intel Corporation, Richard Anderson, Ann Campbell, and Jerry Soden of Sandia National Laboratories, and Charles Hawkins of the University of New Mexico for their careful review of the manuscript. The authors also thank David A. Benson of Sandia for thermal modeling results. Sandia is a multiprogram laboratory operated by Sandia Corporation, a Lockheed Martin Company, for the United States Department of Energy under contract number DE-AC04-94AL85000.

REFERENCES

[1] D.L. Barton, P. Tangyunyong, J.M. Soden, A.Y. Liang, F.J. Low, A.N. Zaplatin, K. Shivanandan, and G. Donohoe, "Infrared Light Emission From Semiconductor Devices", *ISTFA*, 1996, pp. 9-17.

[2] E.I. Cole Jr., J.M. Soden, J.L. Rife, D.L. Barton, and C.L. Henderson, "Novel Failure Analysis Techniques Using Photon Probing in a Scanning Optical Microscope", *IRPS*, 1994, pp. 388-398.

[3] K. Nikawa and S. Inoue, " Various Contrasts Identifiable From the Backside of a Chip by 1.3 μm Laser Beam Scanning and Current Changing Imaging", *ISTFA*, 1996, pp. 387-392.

[4] N.W. Ashcroft and N.D. Mermin, *Solid State Physics*, Philadelphia, Saunders College, 1976, ch. 1, pp. 24-25.

[5] Internet site, http://www.seebeck.com/seebeff.html, referenced 1/7/98.

[6] T. Koyama, Y. Mashiko, M. Sekine, H. Koyama, and K. Horie, "New Non-Bias Optical Beam Induced Current (NB-OBIC) Technique for Evaluation of Al Interconnects", *IRPS*, 1995, pp. 228-233.

[7] E.I. Cole Jr. and R.E. Anderson, "Rapid Localization of IC Open Conductors Using Charge-Induced Voltage Alteration (CIVA)," *IRPS*, 1992, pp. 288-298.

[8] E.I. Cole Jr., J.M. Soden, B.A. Dodd, and C.L. Henderson, "Low Electron Beam Energy CIVA Analysis of Passivated ICs," *ISTFA*, 1994, pp. 23-32.

[9] E.I. Cole Jr., J.M. Soden, P. Tangyunyoug, P.L. Candelaria, R.W. Beegle, D.L. Barton, C.L. Henderson, and C.F. Hawkins, "Transient Power Supply Voltage (v_{DDT}) Analysis for Detecting IC Defects," *ITC*, 1997, pp. 23-31.

[10] Raymond A. Serway, *Physics for Scientists and Engineers with Modern Physics*, second edition, Saunders Publishing Co., NY, 1986, ch. 27, pp. 605-606.

[11] S. Ferrier, "Thermal and Optical Enhancements to Liquid Crystal Hot Spot Detection Methods," *ISTFA*, 1997, pp. 57-62.

[12] S. E. Aw, H. S. Tan, and C. K. Ong, "Optical Absorption Measurements of Band-gap Shrinkage in Moderately and Heavily Doped Silicon", *J. Phys.: Condens. Matter*, **3**, 1991, pp. 8213-8223.

[13] D.L. Barton and P. Tangyunyong, "Fluorescent Microthermal Imaging - Theory and Methodology for Achieving High Thermal Resolution Images," *Microeleronic Engineering*, **31**, 1996, pp. 271-279 .